Differential effects of amyloid-beta 1–40 and 1–42 fibrils on 5-HT1A serotonin receptors in rat brain

Mathieu Verdurand, Fabien Chauveau, Alexia Daoust, Anne-Laure Morel, Frédéric Bonnefoi, François Liger, Anne Bérod, Luc Zimmer

Accepted Manuscript

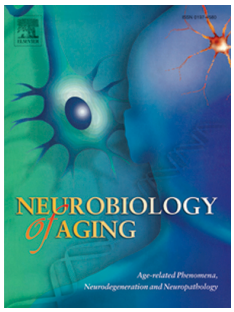

Differential effects of amyloid-beta 1-40 and 1-42 fibrils on 5-HT_{1A} serotonin receptors in rat brain

Mathieu Verdurand, Fabien Chauveau, Alexia Daoust, Anne-Laure Morel, Frédéric Bonnefoi, François Liger, Anne Bérod, Luc Zimmer

PII: S0197-4580(15)00612-0

DOI: 10.1016/j.neurobiolaging.2015.12.008

Reference: NBA 9478

To appear in: *Neurobiology of Aging*

Received Date: 19 March 2015

Revised Date: 8 December 2015

Accepted Date: 15 December 2015

Please cite this article as: Verdurand, M., Chauveau, F., Daoust, A., Morel, A.-L., Bonnefoi, F., Liger, F., Bérod, A., Zimmer, L., Differential effects of amyloid-beta 1-40 and 1-42 fibrils on 5-HT_{1A} serotonin receptors in rat brain, *Neurobiology of Aging* (2016), doi: 10.1016/j.neurobiolaging.2015.12.008.

Differential effects of amyloid-beta 1-40 and 1-42 fibrils on 5-HT_{1A} serotonin receptors in rat brain

Author names and affiliations.
Mathieu Verdurand [a], Fabien Chauveau [a*], Alexia Daoust [a*1], Anne-Laure Morel [a], Frédéric Bonnefoi [b], François Liger [b], Anne Bérod [a], Luc Zimmer [a,b,c]

[a] Université de Lyon ; CNRS UMR5292 ; INSERM U1028 ; Lyon Neuroscience Research Center ; Université Claude Bernard Lyon 1, Lyon, France.
[b] CERMEP-Imaging Platform, Bron, France.
[c] Hospices Civils de Lyon, Lyon, France.

* authors that have contributed equally to this paper.

Corresponding author.
Mathieu Verdurand.
Centre de Recherche en Neurosciences de Lyon, Equipe BIORAN, CERMEP-Imagerie du vivant, 59 boulevard Pinel, F-69677, Bron, France.
Tel: + 33 4 72 68 86 33
Fax: + 33 4 72 68 86 10
E-mail: verdurand@cermep.fr (additional contact, Luc.Zimmer@univ-lyon1.fr)

Present address.
[1] NIH, NINDS, LFMI, FMMS, 10 Center Drive, Building 10, room 1D48, Bethesda, MD, 20892, USA.

ABSTRACT

Evidence accumulates suggesting a complex interplay between neurodegenerative processes and serotonergic neurotransmission. We have previously reported an overexpression of serotonin 5-HT_{1A} receptors (5-HT_{1A}R) following intra-hippocampal injections of amyloid-beta 1-40 (Aβ40) fibrils in rats. This serotonergic reactivity paralleled results from clinical positron emission tomography studies with [^{18}F]MPPF revealing an overexpression of 5-HT_{1A}R in the hippocampus of patients with mild cognitive impairment. Since Aβ40 and Aβ42 isoforms are found in amyloid plaques, we tested in this study the hypothesis of a peptide- and region-specific 5-HT_{1A}R reactivity by injecting them, separately, into the hippocampus or striatum of rats. [^{18}F]MPPF *in vitro* autoradiography revealed that Aβ40 fibrils, but not Aβ42, were triggering an overexpression of 5-HT_{1A}R in the hippocampus and striatum of rat brains after 7 days. Immuno-histochemical approaches targeting neuronal precursor cells, mature neurons and astrocytes showed that Aβ42 fibrils caused more pathophysiological damages than Aβ40 fibrils. The mechanisms of Aβ40 fibrils-induced 5-HT_{1A}R expression remains unknown but hypotheses including neurogenesis, glial expression and axonal sprouting are discussed.

Highlights.

- Neurodegenerative processes have effects on serotonergic neurotransmission
- Aβ40 fibrils, but not Aβ42, can trigger an overexpression of 5-HT_{1A}R in rat brain
- Aβ42 fibrils are more neurotoxic than Aβ40 *in vivo*
- Aβ42 fibrils decrease neurogenesis in the hippocampus

Keywords.

Alzheimer's disease, amyloid-beta peptides, serotonin, 5-HT_{1A} receptors, positron emission tomography.

INTRODUCTION

Alzheimer's disease (AD) is a very complex neuropsychiatric disease where memory becomes progressively dysfunctional resulting in amnesia and dementia. It is the most common cause of dementia worldwide. Neuropathological hallmarks of AD include extracellular deposition of amyloid-beta (Aβ) protein as senile plaques, the gradual intraneuronal accumulation of neurofibrillary tangles formed as a result of abnormal hyperphosphorylation of cytoskeletal tau protein, massive neuronal death (Selkoe, 2001) and relevant neurochemical alterations (Querfurth and LaFerla, 2010). However, most of these pathological studies have been cross-sectional and cannot determine how these key events are temporally related to each other.

Dysfunction of the cholinergic system is usually considered as the most prominent neurotransmitter abnormality but cognitive, behavioural and neuropsychiatric symptoms have been linked to changes in other neurotransmitter systems like the serotonergic (5-HT) one (Assal and Cummings, 2002, Ramirez et al., 2014). Several *post mortem* studies support the involvement of the serotonin system in AD (Meltzer et al., 1998, Rodriguez et al., 2012). Reductions of 5-HT neurons localised in the nucleus raphe dorsalis have been found in AD patient brain samples (Aletrino et al., 1992, Halliday et al., 1992, Zweig et al., 1988). Accordingly, declines in serotonin concentrations (Reinikainen et al., 1990) as well as serotonin reuptake sites (Chen et al., 1996, Cross, 1990, D'Amato et al., 1987) have been observed in target areas of 5-HT projections including the temporal cortex, hippocampus and striatum. A substantial number of *post mortem* studies have also reported reductions in levels of 5-HT_{2A} receptors and 5-HT_{6} receptors (Cross et al., 1986, Lai et al., 2005, Lorke et al., 2006, Reynolds et al., 1984) in the temporal, prefrontal and frontal cortex of AD patients.

5-HT_{1A} receptors (5-HT_{1A}R) are particularly relevant to AD because they are highly expressed in the human hippocampus (Palacios et al., 1990), an important component of the medial temporal lobe memory system, and are known to be involved in the regulation of memory processes (Ogren et al., 2008). The hippocampus is one of the earliest brain regions to be affected by AD neuropathology (Braak et al., 1993). When looking at 5-HT_{1A}R expression in the medial temporal lobe of AD *post mortem* brains, decreased levels (Becker et al., 2014, Bowen et al., 1989) or unchanged density (Becker et al., 2014, Cross et al., 1986, Lai et al., 2003) have been reported. These apparently conflicting results may have arisen from the different techniques and

"markers" used (radiotracers, antibodies), the various stages of the disease (Braak et al., 1993) as well as the particular subregions of the medial temporal lobe assessed.

Interestingly, clinical imaging studies using *in vivo* positron emission tomography (PET) with a selective 5-HT_{1A}R antagonist, fluoro 2'-methoxyphenyl-(*N*-2'-pyridinyl)-p-^{18}F-fluoro-benzamidoethylpiperazine ([^{18}F]MPPF) (Aznavour and Zimmer, 2007, Cheng, 2004) have focused on the status of these receptors in the hippocampus of AD patients at different stages of the disease. While a majority of these studies have shown a decrease of 5-HT_{1A}R density in patients with advanced AD (Kepe et al., 2006, Lanctot et al., 2007), others have reported an increase in the case of patients at pre-dementia stages of AD (Truchot et al., 2008, Truchot et al., 2007). This observation was in accordance with functional magnetic resonance imaging evidence for hyperactivity in the hippocampus before or during the onset of cognitive defects in mild cognitive impairment (Stargardt et al., 2015). One hypothesis to account for these observations is that 5-HT_{1A}R up-regulation may intervene at early stages of AD and may constitute a potential sensitive tool as imaging biomarker of AD as well as an early therapeutic target (Ramirez et al., 2014, Santarelli et al., 2003). Whether the enhanced 5-HT_{1A}R expression during pre-symptomatic stages of AD provides protection against the earliest disease processes or is a pathogenic contribution to AD remains to be determined.

In line with proposals of a 5-HT_{1A}R involvement in cognitive processing, particularly during AD (Bowen et al., 1994), 5-HT_{1A}R antagonists have been developed with the therapeutic aim of enhancing cognitive capacity, though no positive results have been yet reported in clinical trials (Schechter et al., 2005). A study reported the potential beneficial effects of 5-HT_{1A}R agonists in treating non-cognitive symptoms observed in patients with dementia (Sato et al., 2007). Converging preclinical and clinical results are still awaited to confirm the therapeutic promise of 5-HT_{1A}R targeting in AD (Ramirez et al., 2014, Rodriguez et al., 2012).

In a previous preclinical study, we have explored the temporal sequences of changes in hippocampal 5-HT transmission in a rat model of AD with amyloid-beta 1-40 (Aβ40) fibrils deposition in the dentate gyrus (DG) of dorsal hippocampus (Verdurand et al., 2011). We demonstrated a specific, transient 5-HT_{1A}R over-expression that resembled the reactivity observed in the prodromal phase of AD patients (MCI or mild cognitive impairment) (Truchot et al., 2008, Truchot et al., 2007) associated with a substantial loss of granular glutamatergic neurons.

However, although the Aβ40 peptide is consistently found in the senile plaques of AD *post mortem* patients' brain, it is usually co-localized with the Aβ42 peptide (Klein et al., 1999) which has consistently demonstrated high neurotoxic effects in neuronal cultures (Dahlgren et al., 2002) and when injected in rodents brains (Klein et al., 1999). In this context, our study was designed i) to compare the early effects of Aβ40 or Aβ42 fibrils deposition on 5-HT_{1A}R expression across two brain regions where prominent amyloid deposition can be observed in pre-symptomatic AD, the hippocampus and the striatum, and ii) to explore the cellular events that operate early after Aβ depositions. To that aim, brain sections were immunostained with a neuron-specific nuclear protein (NeuN), a pan-neuronal marker, double-cortin (DCX) a marker transiently expressed by newly generated neurons, and Glial Fibrillary Acidic Protein (GFAP), a protein marker for astrogliosis.

2. MATERIALS AND METHODS

2.1. Preparation of the amyloid-beta (Aβ) fibrils

Methods for preparation and aggregation of the peptides were derived from previous studies (Bagheri et al., 2011, Verdurand et al., 2011, Wu et al., 2007). Human recombinant amyloid-beta peptides 1-40 (Aβ40) (Sigma-Aldrich, France) were dissolved in Tris-Buffered Saline supplemented with HCl (TBS-HCl) (Sigma-Aldrich; 138 mM NaCl, 2.7 mM KCl, pH adjusted to 7.5) at a concentration of 100 µM and aliquots of 100 µL were kept at -80°C. Human recombinant amyloid-β peptides 1-42 (Aβ42) (Bachem, Switzerland) were dissolved in TBS-HCl supplemented with NH_4OH at a concentration of 100 µM and aliquots of 20 µL were stored at -80°C. Aggregation of peptides consisted in placing aliquots at 37°C under agitation (250 rpm; Thermo-Shaker, PHMT, GrantBio) for at least 2 days.

2.2. Transmission Electronic Microscopy (TEM)

TEM was used to detect the presence of fibrils. 3 µL of fibril sample were absorbed on 200 mesh nickel grids coated with formvar-C for 2 min at room temperature (RT). A torn edged of hardened, ashless filter paper was applied at the edge of the grid to absorb the remaining liquid. Then, 3 µL of 3% uranyl acetate in distilled de-ionized water was added to the grid for 1 min, excess was wicked away and the grid allowed to air dry before examination using a transmission

electron microscope (Jeol JEM 1400, Tokyo, Japan) operating at 80 kV equipped with a numeric camera (GATAN Orius 600, Evry, France). The images were processed by Digital Micrograph (Figure 1).

2.3. Animals

Seventy-one adult male Sprague-Dawley rats (8-9 weeks old) weighing 250-350g were used (Charles River Laboratories, L'Abresle, France). The animals were kept at a constant temperature of 22 ± 2°C on a 12-12 h light-dark cycle with lights on at 9 am. All animal experiments were performed in accordance with the European guidelines (2010/63/UE) and subsequent national decree (2013-118) for care of laboratory animals, and were approved by the Animal Use Ethics Committee of the University of Lyon (C2EA – 42; Comité d'éthique en Expérimentation Animale Neurosciences Lyon; celyne.lyon@inserm.fr).

2.4. Intracerebral injections of Aβ fibrils in rats

Rats were anaesthetized with isoflurane inhalation in air (4% isoflurane in 1 L/min air) and then transferred to a stereotaxic apparatus (Stoelting, USA) equipped with a mask delivering isoflurane at 1.5-2.5% in air flow set at 0.5-0.6 L/min for the duration of the experiment. The eyes were coated with a lubricating eye ointment. Body temperature was maintained by a heating pad (CMA/microdialysis 150) set at 37°C and monitored rectally. A pulse oximeter (NONIN Medical, USA) was used to measure heart rate (350 ± 50 beats/min), respiratory rate (45 ± 15 cycles/min) and oxygen saturation (>90%). Because of the invasive nature of the surgery performed (brain stereotaxic injections), pain was controlled by the potent opioid analgesic buprenorphine (Buprecare®, Axience) injected subcutaneously (s.c.) at a dose of 0.05 mg/kg, 20 min before any surgical act was performed.

Animals were stereotaxically injected with pre-aggregated amyloid peptides (0.5 nmol in 5 µL per injection site), according to the stereotaxic atlas of the rat brain (Paxinos and Watson, 2007). Incision was performed on the scalp of the rats in order to visualise the bregma anatomical point (intersection of coronal and sagittal suture). Aβ40 and Aβ42 were unilaterally injected in the dentate gyrus of dorsal hippocampus (vehicle in the contralateral hemisphere, n = 36) at the following stereotaxic coordinates relative to bregma: AP = -3.2 mm; ML = ±1.2 mm; DV = -3.6 mm. In a separate cohort of rats (n = 35), Aβ40 and Aβ42 were unilaterally injected in the

striatum (vehicle in the contralateral hemisphere) at the following coordinates relative to bregma: AP = 0.1 mm; ML = ±3.3 mm; DV = -4.2 mm.

Aβ40, Aβ42 fibrils and vehicle solutions (5 µL each) were slowly infused at a constant rate of 1 µL/min by a home-made system consisting of Hamilton syringes (1702 SN, NHBIO, France) installed in injection pumps (World Precision Instruments, UK), connected via a tubing (Fine Bore Polythene Tubing, Portex, Smith Medical Intl, UK) to Hamilton needles of 30 Gauge diameter (RN, NH BIO, France). The needles were left in place for 2 min and then slowly withdrawn. After injections, the scalp was sutured, an antiseptic (povidone-iodine) and local analgesic (lidocaine) applied, and the rats were allowed to recover from anaesthesia. A 7 days post-injection delay was observed before euthanasia and subsequent studies.

2.5. *In vitro* [^{18}F]MPPF autoradiography experiments and data analysis

Following a 7 days post-injection period (n=6 for each group of rats), rats were deeply anaesthetized with isoflurane in the inducing chamber (4% isoflurane in 1L/min air flow) and rapidly euthanized by decapitation. Brains were dissected and frozen in 2-methylbutane with dry ice (-30°C). Twenty µm-thick sections were cut across the injected regions of interest (dorsal hippocampus and striatum), thaw-mounted on slides (Superfrost®, Roth, France) and allowed to air-dry for 30 min before storage at -80°C until use. *In vitro* autoradiography experiments were performed with [^{18}F]MPPF, a specific 5-HT$_{1A}$R PET radiotracer (Le Bars et al., 1998). On the day of [^{18}F]MPPF radiosynthesis, the slides were allowed to thaw to room temperature (30-60 min) and the sections were incubated at room temperature for 20 min in Tris-buffered saline (TBS) supplemented with HCl (TBS-HCl buffer) (138 mM NaCl, 2.7 mM KCl, pH adjusted to 7.5) containing a 5-HT$_{1A}$R saturating concentration of [^{18}F]MPPF (≥ 3 nM, ≥ 3 times Kd). Adjacent sections were incubated in the same medium supplemented with 10 µM of WAY-100635 (5-HT$_{1A}$R antagonist, Sigma-Aldrich, France) to estimate the non-specific binding. After 20 min of incubation, the slides were washed for 90 sec in cold TBS-HCl buffer, rinsed for 90 sec in cold distilled water, dried under cool air and exposed to sensitive imaging plates (BAS-IP MS 2025, Fujifilm) for 60 min. The distribution of radioactivity was then visualized with a Bio-imaging analyser system (BAS-5000, Fujifilm) and analysed using the Multigauge software (Fujifilm). Regions of interest were manually drawn in the targeted injection sites (24 sections

per animal), namely the dentate gyrus of the dorsal hippocampus and the striatum, with the help of a stereotaxic atlas of the rat brain (Paxinos and Watson, 2007).

Semi-quantitative [^{18}F]MPPF binding values were expressed in psl/mm^2 (photo-stimulated luminescence per surface unit). Non-specific [^{18}F]MPPF binding values (measured from adjacent slices) were subtracted to total [^{18}F]MPPF binding ones to obtain the specific 5-HT_{1A}R regional density. Specific [^{18}F]MPPF binding means were calculated as percentage of change (% change) between the Aβ-injected and the contralateral vehicle-injected regions (mean value for the 6 vehicle injections was set to 100%).

2.6. Quantitative real-time PCR (qRT-PCR) experiments and data analysis

Following a 7 days post-injection period (n=6 for each group of rats), rats were deeply anaesthetized with isoflurane in the inducing chamber (4% isoflurane in 1L/min air flow) and rapidly euthanized by decapitation. The dorsal hippocampus and striatum regions were manually dissected on ice and stored at -80°C before use. RNA was isolated on silica-based columns, DNase I digested and eluted with water, using RNeasy Mini Kit following the manufacturer's instructions (Qiagen, France). Total RNA was quantified using DO 260 nm on a NanoDrop 1000 spectrophotometer (ThermoScientific, Baltimore, MA, USA) and quality was assessed with the Agilent 2100 Bioanalyser (Agilent Technologies, Palo Alto,CA, USA). RNA (750ng) was reverse transcribed using the iScript Reverse Transcription Supermix (Bio-Rad, Hercules, CA, USA). The expression of conventionally used house-keeping genes including Ywhae, RPL4, GAPDH proved to be stable between assays. Quantitative real-time PCR (qRT-PCR) was performed with the Fast SYBR Green Master Mix and the Applied Biosystems 7900HT Fast Real –Time PCR system (Appied Biosystems, Foster city, California USA). The experimental protocol consisted of an initial polymerase activation at 95 °C, for 20 min followed by an amplification program for 40 cycles keeping the annealing and extension primer temperature at 62 °C for 20min. Melting-curve analysis was then performed to verify the amplification of a single product. All primers were designed using NCBI Primer-BLAST and selected to generate amplicons with a length of 100–200 bp. The primer sequences used in this study were as followed (5' AAG-AAG-AGC-CTG-AAC-CGA-CA 3' (forward) and 5' CAG-AGG-AAG-GTG-CTC-TTT-GG 3' (reverse) for 5-HT_{1A}R). Standard curves were generated for each primer set to calculate the efficiency of each set. Only primer sets with an efficiency of 1.85 to 2.1 were used for qPCR. The

relative mRNA levels for each assay were computed from the C_t (cycle threshold) values obtained for the target gene. qPCR experiments were repeated at least three times using independent RNA/cDNA preparations. Data was pooled and analysed using RQ manager v1.2 and dataAssist v1.0 (Applied Biosystems). For each injection, RQ value (relative quantitation (RQ) or fold change) was normalized to the mean value of the vehicle injections in the corresponding region.

2.7. Thioflavine S histological staining

Thioflavine S (Sigma-Aldrich, France) staining was performed to confirm the presence of aggregated amyloid material at the site of injection. Brain sections were rinsed twice in PBS for 10 min, incubated in thioflavine S 0.0025% for 8 min, then 1 min in ethanol 80%, 1 min in ethanol 50% and 10 min in PBS before mounting in aqueous mounting medium with DAPI (Vectashield Hardset Mounting Medium with DAPI, Vector Labs, Eurobio, France). The induced fluorescence was observed using an imaging microscope (Axioplan-2, Zeiss; Oberkochen, Germany). The filter used was FITC (ex 470 ± 20 nm, em >515 nm). Images were captured using a digital camera interfaced with image-analysis computer (Axiovision 3.0 software, Zeiss).

2.8. Immunohistochemical staining (NeuN, GFAP, DCX) and quantification

For immunohistochemistry, rats (hippocampus: n=7 for Aβ40 and n=6 for Aβ42; striatum: n=5 for Aβ40 and n=6 for Aβ40) were deeply anaesthetized with pentobarbital (50 mg/kg i.p.) and perfused transcardially with paraformaldehyde (4%) in PBS. The brains were post-fixed overnight, cryoprotected with 30% sucrose for 48h at 4°C, frozen in 2-methylbutane supplemented with dry ice to reach -30°C, and stored at -20°C. Free-floating coronal sections (30 µm thick) were processed using a standard avidin-biotin-peroxydase method as previously described (Verdurand et al., 2011). Briefly, one-in-six series of free-floating tissue sections were taken for each rat and incubated overnight at room temperature with primary specific antibodies directed against GFAP (rabbit antibody, Dako, Carpinteria, CA; 1/10000 dilution), DCX (polyclonal goat antibody IgG, Santa Cruz Biotechnology, CA; 1/2000) and NeuN (monoclonal mouse antibody IgG, Millipore; 1/10000 dilution). Bound antibodies were visualized using biotinylated secondary antibody (for GFAP: biotinylated goat anti-rabbit antibody; Vector Laboratories Inc., Burlingame, CA; 1/1000 dilution; for DCX: biotinylated horse anti-goat antibody, 1/1000 dilution; for NeuN: biotinylated horse anti-mouse antibody, 1/1000 dilution).

Quantification strategy for DCX, NeuN and GFAP staining in the dorsal dentate gyrus

Bright field images of sectioned material were viewed with a Zeiss Axioskop 2 microscope equipped with an X/Y sensitive stage and a video camera connected to a computerized image analysis system (Mercator, Explora Nova, France). The planes of the analyzed sections were standardized according to the atlas of Paxinos and Watson (1998). The quantification for DCX and NeuN staining was carried out in 8 sections starting from the appearance of the dorsal dentate gyrus. These sections were in intervals of one-in-6 series of sections, therefore 150 µm apart.

For evaluation of the Aβ40 or Aβ42-induced lesions in the dentate gyrus 8 sections, the NeuN staining area in the supragranular and infragranular blades of the dorsal dentate gyrus was delineated at low magnification (x 2.5 objective). The total NeuN staining area in the dentate gyrus was calculated using Mercator software. As an index of lesion severity, the reduction of NeuN positive area in the dentate gyrus (ipsilateral to amyloid peptide injection) was calculated as a percentage of the PBS injected contralateral side.

DCX-labeled cells were counted manually by an observer blind to the experimental groups under a x 20 objective. The number of DCX cells in the dentate gyrus was summed on each side and change induced by the amyloid fibrils (ipsilateral to amyloid peptide injection) was calculated as a percentage of the PBS injected contralateral side.

Astrocyte reactivity (astrogliosis) around the injection site was evaluated with a semi-quantitative method. Under a x 5 objective, contra vs ipsilateral GFAP staining were visually evaluated on each (hippocampal and striatal) injection sites and scored by a blind observer as follows: 0, sparse reactivity; 1, strong reactivity on a localized, small area; 2, strong reactivity on a large area. Scores were summed across each hemisphere to yield a semi-quantitative measure of glial reactivity for each injection.

Quantification strategy for NeuN and GFAP staining in the striatum

In the striatum, a different quantitative approach was undertaken with delineation of NeuN lesion volume as opposed to the evaluation of remaining NeuN staining for the dentate gyrus. This method was better adapted to the weak NeuN staining in the striatum compared to that of the hippocampus, where manual counting would be poorly reliable. Tissue sections were analyzed under a x 5 objective and areas devoid of staining were manually outlined across the injection site

in the striatum (typically 4-8 sections with 150 µm inter-section distance) by an observer blind to the experimental groups. Areas were interpolated to yield a total volume of neuronal loss expressed in mm^3.

Astrocyte reactivity (astrogliosis) around the injection site was visually evaluated as in the hippocampus (score 0-2 on each hemisphere).

2.9. Statistical analysis

All statistical analysis were conducted in GraphPad Prism 5, with a p value <0.05 considered statistically significant. For autoradiography, qRT-PCR, DCX and NeuN data, differences between ipsilateral (Aβ-injected) and contralateral (vehicle-injected) hemispheres were analysed for statistical significance by paired, one-tailed Student's t-test. Wilcoxon matched-pairs signed rank test (non-parametric, paired) was used for comparison of GFAP scores.

3. RESULTS

3.1. Transmission Electron Microscopy (TEM)

Aβ aggregates observed by TEM with uranyle acetate negative staining clearly demonstrated the presence of fibrils for both Aβ40 and Aβ42 peptides (Figure 1). Structures of 5-10 nm width typical of Aβ fibrils could be seen, linear and unbranching (Nilsson, 2004). However, a different overall aspect was observed between Aβ40 and Aβ42. Indeed, Aβ40 fibrils appeared wider and laterally associated. Aβ42 fibrils appeared thinner and few grown in parallel. While Aβ40 fibrils were longer and ramified, Aβ42 were shorter and well separated.

3.2. Thioflavine S

Thioflavine S staining of amyloid fibrils, combined with DAPI staining of cell nuclei, confirmed the presence of aggregated material in the dentate gyrus of dorsal hippocampus as well as in the striatum, on the site of Aβ40 and Aβ42 fibrils injections (Figure 2).

3.3. Aβ40, but not Aβ42 fibrils, increase 5-HT_{1A}R binding in the dentate gyrus and striatum

At 7 days post-injection, Aβ40 fibrils infused in the dentate gyrus of hippocampus (634.0

± 42.1 psl/mm^2) triggered a significant increase in specific [^{18}F]MPPF binding (+40.9%, t(5) = 5.917, p = 0.001) around the injection site in comparison to the vehicle injected contralateral side (449.7 ± 26.1 psl/mm^2). A significant increase in [^{18}F]MPPF binding (+20.7%, t(5) = 6.263, p < 0.001) was also observed in the striatum injected with Aβ40 fibrils (38.3 ± 1.3 psl/mm^2) in comparison to the vehicle injected contralateral side (31.7 ± 1.2 psl/mm^2) (Figure 3).

By contrast, injection of Aβ42 fibrils in the dentate gyrus of dorsal hippocampus (Aβ42: 1327.0 ± 117.7 psl/mm^2, +7.9% vs vehicle injected contralateral side 1230.0 ± 125.4 psl/mm^2, t(5) = 0.936, p= 0.196) or the striatum (Aβ42: 41.5 ± 2.1 psl/mm^2, +3.1% vs vehicle injected contralateral side 40.2 ± 2.4 psl/mm^2, t(5) = 0.841, p = 0.219) did not affect [^{18}F]MPPF binding (Figure 3).

3.4. Aβ42 fibrils decrease 5-HT$_{1A}$ mRNA expression in the hippocampus

We then analysed the expression of 5-HT$_{1A}$ mRNA in the dorsal hippocampus and striatum. At 7 days post-injection, Aβ40 fibrils infused in the dentate gyrus of hippocampus (1.3 ± 0.1 relative quantitation (RQ)) did not trigger any significant change in 5-HT$_{1A}$ mRNA expression (-0.7%, t(5) = 0.080, p = 0.470) in comparison to the vehicle injected contralateral side (1.3 ± 0.2 RQ). No significant change in 5-HT$_{1A}$ mRNA expression (+95.5%, t(5) = 1.210, p = 0.141) could be observed in the striatum injected with Aβ40 fibrils (1.7 ± 1.3 RQ) in comparison to the vehicle injected contralateral side (0.9 ± 0.4 RQ) (Figure 4).

However, after injection of Aβ42 fibrils in the dentate gyrus of dorsal hippocampus (1.0 ± 0.3 RQ), a significant decrease in 5-HT$_{1A}$ mRNA expression (-22.9%, t(5) = 2.164, p= 0.041) could be observed in comparison to the vehicle injected contralateral side (1.3 ± 0.2 RQ). Aβ42 injected in the striatum (2.6 ± 1.9 RQ) did not have any significant effect on 5-HT$_{1A}$ mRNA expression (+159.8%, t(5) = 1.900, p = 0.058) in comparison to the vehicle injected contralateral side (0.9 ± 0.4 RQ) but showed a decreased trend in 5-HT$_{1A}$ mRNA expression, an effect opposite to that observed in the hippocampus (Figure 4).

3.5. Aβ42 fibrils are more neurotoxic than Aβ40 fibrils *in vivo*

3.5.1. Dorsal hippocampus

To specifically examine neuronal loss in the dentate gyrus, NeuN immunohistochemistry and regional brain analysis was performed. Injections of Aβ40 and Aβ42 fibrils in the dorsal dentate

gyrus revealed a clear loss of granular cell in the dentate gyrus that was more marked with Aβ42 fibrils (Figure 5). Evaluation of the percentage loss of neurons in the dentate gyrus suggested the higher neurotoxicity of Aβ42, since the mean loss of NeuN staining was not significantly different after Aβ40 fibrils injection but tended to decrease (-20.2%) after Aβ42 fibrils injection (surface of NeuN staining in vehicle injected rats 204192 ± 26498 μm^2 vs 162908 ± 31197 μm^2 when Aβ42 fibrils were injected, $t(4) = 1.108$, $p = 0.165$) (Figure 5).

In order to determine if these two peptides have a differential effect on newly born granular cells, a regional analysis of DCX-expressing cells was performed. As expected, DCX-positive cells in the hippocampus were confined to the sub-granular zone, immediately adjacent to both the supra-granular and infra-granular blades of the dentate gyrus. DCX-immunoreactivity extended from the perikarya to the developing dendritic arbors in the molecular layer (Figure 5). Quantification of DCX positive neurons in the dentate gyrus revealed no significant changes (+2.6%, $t(6) = 0.323$, $p = 0.379$) in the Aβ40-injected hemisphere (1321 ± 133 DCX+ cells/DG) in comparison to the vehicle-injected contralateral side (1287 ± 149 DCX+ cells/DG). Interestingly, when Aβ42 fibrils were injected (1149 ± 127 DCX+ cells/DG), a significant decrease in DCX positive cells (-24.7%, $t(4) = 6.824$, $p = 0.001$) was observed in comparison to the vehicle injected hemisphere (1526 ± 88 DCX+ cells/DG).

Astrogliosis, revealed by GFAP immunostaining, was apparent and more important in the dentate gyrus injected with Aβ42 fibrils than in Aβ40 injected hemispheres and finally mildly apparent in the vehicle-injected contralateral sides (mechanical damages) (Figure 5). However, scores analysis of the astroglial reaction does not indicate a clear differential effect of Aβ40 and Aβ42. Indeed, astroglial reaction triggered by Aβ40 (median score [min;max] = 7[2;16]) was not significantly different ($p = 0.500$) from the scores obtained in the vehicle injected hemispheres (median score = 9[4;13]). Similarly for Aβ42 (median score = 14[6;20]), there was no significant reaction ($p = 0.170$) in comparison to the vehicle-injected hemispheres (median score = 10[1;15]), despite a clear trend toward higher scores.

Altogether, these results indicate that Aβ42 fibrils injections in the dentate gyrus have a more pronounced neurotoxic effect on mature and newly born neurons of the granular cell layer than Aβ40 fibrils.

3.5.2. Striatum

Because of the size of the striatum and the weak labeling of NeuN-expressing cells in this brain structure, extension of neuronal loss through NeuN staining was analyzed differently. Delineation of NeuN lesion volume as opposed to the evaluation of remaining NeuN staining for the dentate gyrus was performed (Figure 6). In the striatum, a non-significant trend in increase in lesion volume (+55.1%, $t(5) = 1.828$, $p = 0.071$) was observed after Aβ40 fibrils injections (0.0664 ± 0.0133 mm^3) in comparison to vehicle injected hemispheres (0.0428 ± 0.0071 mm^3). Additionally, a significant increase (+212.7%, $t(5) = 2.985$, $p = 0.015$) in lesion size was observed after Aβ42 fibrils injections (0.1817 ± 0.0459 mm^3) in comparison to the vehicle injected contralateral hemisphere (0.0582 ± 0.0957 mm^3).

DCX-immunoreactive cells were observed in the rostral migratory stream, where neuronal precursors migrate from the sub-ventricular zone of the lateral ventricles towards the olfactory bulb. No specific DCX labelling was apparent in the striatum parenchyma and at the site of injection thus no quantification was performed in this brain area (Figure 6).

For astrogliosis evaluation in the striatum, Aβ40 fibrils (median score [min; max] = 15[10;17]) did not trigger any significant astroglial reaction ($p = 0.500$) in comparison to the vehicle injected hemisphere (median score = 14[11;22]). However, 7 days after Aβ42 fibrils injection (median score = 14[11;16]), a significant increase ($p = 0.029$) in GFAP staining was observed in comparison to the vehicle injected contralateral side (median score = 10.5[6;13]).

As observed in the dentate gyrus, Aβ42 fibrils are more neurotoxic in the striatum than Aβ40 fibrils.

4. DISCUSSION

Our study demonstrated that Aβ40 and Aβ42 fibrils injections in the brain trigger different cellular events, at least early after their deposition. In particular, we demonstrated that Aβ40 fibrils injections were capable of triggering an up-regulation of 5-HT_{1A}R binding in the rat hippocampus and striatum while Aβ42 fibrils were not. Apart from a differential regulation of 5-HT_{1A}R binding, the present study also identified more pathophysiological damage after Aβ42 fibrils injection than Aβ40. Notably, this was evidenced by a trend or a significant loss of mature neuron in the hippocampus and striatum respectively, a strong reactive astrogliosis as well a significant decrease in newly born granular cells in the dentate gyrus.

Our study first confirmed previous results showing that Aβ40 injected in the hippocampus can trigger 5-HT_{1A}R reactivity 7 days after their injection (Verdurand et al., 2011). As mentioned previously, this observation parallels the *in vivo* [^{18}F]MPPF PET results obtained in patients with mild cognitive impairment (MCI) showing an increased 5-HT_{1A}R density potentially reflecting compensatory mechanisms trying to fight Aβ-induced neurotoxicity that is then overwhelmed at late/advanced AD stages (Kepe et al., 2006, Mizukami et al., 2011, Truchot et al., 2008, Truchot et al., 2007). Interestingly, our study demonstrated a similar effect in the striatum, a region with very low basal 5-HT_{1A}R expression (Palacios et al., 1990) and no intrinsic synthesis of this receptor in basal conditions (Pompeiano et al., 1992). A remarkably high striatal retention of [^{11}C]PIB, an amyloid radioligand, has been observed in familial AD cases known for their early onset and rapid progression of the disease (Klunk et al., 2007, Koivunen et al., 2008, Villemagne et al., 2009). Aβ deposition in the striatum of sporadic AD cases has also been demonstrated to be correlated to Aβ levels in cortical regions (Ishibashi et al., 2014). Moreover, *in vivo* amyloid imaging of the striatum has recently been suggested to be a useful predictor of Braak neuro-fibrillary tangles (NFT) stage and the presence or absence of dementia and clinicopathological AD (Beach et al., 2012). The striatum is thus not completely devoid of implication in AD. However, to our knowledge, an enhanced 5-HT reactivity (5-HT_{1A}R binding or [^{18}F]MPPF binding) has never been investigated and observed in the striatum of AD patients.

Another relevant finding in our study is that Aβ40 fibrils, but not Aβ42, have the potential to trigger a rapid 5-HT_{1A}R reactivity i.e. 7 days after their intracerebral injections. This effect was, at first, unexpected given that Aβ42 are usually described in the literature as having severe neurotoxic effects in animal models of AD (Klein et al., 1999, Zheng et al., 2013) as well as in *in vitro* models (Pike et al., 1993). One could expect that the more neurotoxic peptide form will be the one being the more pathophysiologically "active" when injected *in vivo*. Indeed, in our animal model, immunostaining of specific markers confirmed that Aβ42 fibrils are more neurotoxic than Aβ40 ones. Aβ42 fibrils triggered significant lesion (NeuN immunoreactivity) and astroglial reaction (GFAP immunoreactivity) in the striatum as well as a significant decrease in hippocampal DCX-expressing cells, a good indication of decreased neurogenesis (Couillard-Despres et al., 2005). Therefore during the progress of AD pathology, Aβ42 fibrils may contribute to neuronal loss not only through toxicity toward mature neurons but also through a decrease in neurogenesis. Despite these severe pathophysiological consequences, Aβ42 fibrils did

not have any significant consequences on 5-HT_{1A}R binding when injected in the hippocampus or striatum. And Aβ40 fibrils injections, despite having less significant pathophysiologiocal consequences, were capable of triggering this 5-HT_{1A}R overexpression.

In the search of an explanation for the up-regulation of 5-HT_{1A}R binding following Aβ40 fibrils injections, but not observed after Aβ42, we examined the expression of the corresponding mRNA. Our data showed that the increase in 5-HT_{1A}R binding observed in the hippocampus and striatum following Aβ40 fibrils injections was not accompanied by a concomitant increase in mRNA expression as observed with qRT-PCR. Conversely, the changes in 5-HT_{1A} mRNA levels observed in the hippocampus and striatum after Aβ42 fibrils injection were not converted in 5-HT_{1A}R binding changes.

Aside from technical explanations such as differences in sensitivity and anatomical resolution of qRT-PCR and receptor autoradiography, several hypotheses can be put forward to explain the discrepancies between 5-HT_{1A}R mRNA expression and 5-HT_{1A}R binding. Although it is generally accepted that 30 to 85% of the variation in protein levels can be attributed to variation in mRNA expression, there is still 15 to 70% of the variation that is explained by post-transcriptional and post-translational regulation and by measurements errors (de Sousa Abreu et al., 2009, Maier et al., 2009, Payne, 2015, Vogel and Marcotte, 2012). It is thus possible that unchanged 5-HT_{1A} mRNA levels and enhanced 5-HT_{1A} protein levels that we observed correspond to an enhanced translation of pre-existing 5-HT_{1A} mRNA with no change in transcription. Pathologically elevated Aβ levels triggers a multitude of cellular events including, not only cell death, but also structural and functional changes at the synaptic level and intense astrogliosis (Mucke and Selkoe, 2012). Although still under debate, it has been postulated that astroglial cells may express 5-HT_{1A}R (Hirst et al., 1998, Kia et al., 1996, Patel and Zhou, 2005, Whitaker-Azmitia et al., 1993). In our animal model, an astroglial reaction (although not significant) could be observed on the site of Aβ40 fibrils injections thus prompting us to hypothesize that astrocytes were potentially holding these over-expressed 5-HT_{1A}R. However, the fact that Aβ42 fibrils triggered a significant astroglial reaction in the striatum without a parallel 5-HT_{1A}R overexpression argues against the expression of 5-HT_{1A}R on these cell types. It is unknown whether neural progenitor cells can actually express 5-HT_{1A}R but, in our animal model, the hypothesis of 5-HT_{1A}R expressed by newly generated neurons after Aβ40 fibrils injections can be excluded as neurogenesis revealed to be unchanged (hippocampus) or inexistent

(striatum). Finally, experimental evidence has clearly demonstrated a large sprouting of 5-HT fibres in the hippocampus of mice models of AD (Noristani et al., 2010) or following neurotoxic lesions, a phenomenon likely to occur in our experimental conditions since Aβ40 fibrils injected in the striatum enhanced 5-HT neurotransmission (Verdurand et al., 2011). In basal conditions, 5-HT_{1A}R are essentially addressed to the membrane of soma and dendrites of 5-HT and non-5-HT neurons but not found on the membrane of pre-terminal axons (Pompeiano et al., 1992, Riad et al., 2000). It is however not known if, under pathological conditions, 5-HT_{1A}R can be expressed in 5-HT nerve terminals and, through their potential expression on sprouting fibres, could have contributed to the observed 5-HT_{1A}R binding increase. How these different "partners" contribute to Aβ-induced 5-HT_{1A}R regulation is an important issue to be addressed in the future, considering the importance of these early changes in the development of AD, the potential therapeutic window as well as diagnosis tool they represent.

5. CONCLUSION

In this study, we have demonstrated that 7 days after their stereotaxic injections in rat brains, Aβ40 fibrils, but not Aβ42, were capable of triggering an overexpression of 5-HT_{1A}R in the hippocampus and striatum. In order to investigate the origin of this 5-HT_{1A}R overexpression and the differences obtained with the two fibrils forms, immuno-histochemical approaches allowed us to better characterize the cellular events occurring at the sites of both Aβ40 and Aβ42 injections. We observed that Aβ42 fibrils caused more pathophysiological damages than Aβ40 when injected *in vivo*. These two aspects, 5-HT_{1A}R overexpression with low neuronal loss, re-inforce the value of this simple, non-transgenic animal model as a prodromal model of AD. The mechanisms underlying Aβ40 fibrils induced 5-HT_{1A}R expression remains unknown but the hypothesis of neuronal "sprouting" deserve further attention. Finally, this study gives new argument in favour of the differential dosage of Aβ40 and Aβ42 peptides in human *post-mortem* brain tissue for the stratification and association between molecular changes in AD and their clinical expressions.

ACKNOWLEDGMENTS

Dr Mathieu Verdurand was supported by a Young Researcher Grant from the Fondation Plan Alzheimer (Paris). Elisabeth Errazuriz-Cerda is acknowledged for her assistance in Transmission Electronic Microscopy acquisition and interpretation (Centre d'Imagerie Quantitative Lyon-Est). Catherine Rey of the ProfileXpert-LMCT platform of Lyon University is acknowledged for the qRT-PCR experiments. This work was performed within the framework of the LABEX PRIMES (ANR-11-LABX-0063) of Université de Lyon, within the program "Investissements d'Avenir" (ANR-11-IDEX-0007) operated by the French National Research Agency (ANR) and thanks to a research grant with Fondation Caisse d'Epargne Rhône-Alpes.

FIGURE LEGENDS

Figure 1. Representative transmission electronic microscopy (TEM) images obtained with Aβ40 (left) and Aβ42 (right) pre-aggregated solutions. Uranyle acetate 3% was used for negative staining. Fibrils are clearly visible for both peptides with structures of 5-10 nm width. Aβ40 fibrils appear wider, parallel and long. Aβ42 fibrils appear thinner and shorter. Scale bars represent 100 nm in both images.

Figure 2. Schematic representations of the intracerebral stereotaxic injections in the rat dentate gyrus of dorsal hippocampus or the striatum. Representations were extracted from the stereotaxic atlas of the rat brain (Paxinos and Watson, 2007). Thioflavine S (green) and DAPI (blue) fluorescence staining images are also represented below for both the hippocampus and the striatum. Thioflavine S fluorescence highlights the site of aggregated Aβ injections and is clearly visible in the granular cell layer of the dentate gyrus and in the striatum.

Figure 3. [^{18}F]MPPF *in vitro* autoradiographic images and scatter plots (expressed as [^{18}F]MPPF binding percentage of change relative to the vehicle injected site) obtained in the dentate gyrus of dorsal hippocampus and striatum of Aβ injected rat brains. Manually drawn regions of interest are shown in red for both the dentate gyrus and the striatum. Aβ40 injected animals showed a significant 5-HT$_{1A}$R overexpression represented by increased [^{18}F]MPPF binding level (red arrows) in comparison to the vehicle injected contralateral side.

Figure 4. Quantitative real-time PCR (qRT-PCR) scatter plots results of 5-HT$_{1A}$ mRNA relative expression (expressed as percentage of change relative to the vehicle injected site) in both the hippocampus and striatum after Aβ40 or Aβ42 fibrils injections. A significant decrease in 5-HT$_{1A}$ mRNA expression was observed in the hippocampus 7 days after Aβ42 fibrils injections.

Figure 5. Immuno-histological microscopic images (NeuN, DCX, GFAP) and corresponding scatter plots results of quantifications obtained in the hippocampus of vehicle, Aβ40 and Aβ42 injected hemispheres at 7 days post-injection. NeuN staining showed a slight decrease in the granular cell layer of the dentate gyrus after Aβ40 and a strong decrease after Aβ42 fibrils injections (although not significant). Red dashed arrows represent the extent of NeuN staining

disappearance in the granular cell layer of the dentate gyrus. DCX staining revealed no overall changes in the Aβ40 injected hemispheres. However, a discontinuation in DCX positive cells in the granular cell layer of Aβ42 injected hippocampus was visible. Quantification of DCX staining (number of DCX+ cells in dentate gyrus expressed as percentage of change relative to vehicle injections) revealed a significant decrease in neurogenesis 7 days after Aβ42 fibrils injections (magnified images are provided). A slight increase in GFAP staining in the dentate gyrus of Aβ40 injected animals was observed (red arrows) while an intense GFAP staining could be observed in the Aβ42 injected hemispheres. GFAP staining semi-quantitative score (based on visual observation) could not pick-up any significant changes in the astroglial reaction 7 days after Aβ40 or Aβ42 fibrils injections in comparison to the vehicle injected hemispheres. Scale bars represent 200 µm.

Figure 6. Immuno-histological microscopic images (NeuN, DCX, GFAP) and corresponding scatter plots results of quantifications obtained in the striatum of vehicle, Aβ40 and Aβ42 injected hemispheres at 7 days post-injection. NeuN staining revealed the extent of Aβ induced neurotoxicity. A slight lesion could be observed in the striatum after Aβ40 and a stronger one after Aβ42 fibrils injections. Red dashed delineations represent the extent of the neurotoxic lesion in the striatum. Quantification of NeuN lesion size (expressed in percentage of change relative to vehicle injections) corroborated the visual impression with a significant increase in lesion after Aβ42 injections. DCX staining was present in the known neurogenic sub-ventricular zone (white arrows). However, no specific DCX positive cells were observed in the striatum where Aβ fibrils were injected, thus no quantification was performed. A slight increase in GFAP staining in the striatum of Aβ40 injected animals was observed (red arrows) while a more intense GFAP staining could be observed in the Aβ42 injected hemispheres. GFAP staining semi-quantitative score (based on visual observation) revealed a significant increase in astroglial staining 7 days after Aβ42 fibrils injections in comparison to the vehicle injected hemispheres. Scale bars represent 200 µm.

REFERENCES

Aletrino, M.A., Vogels, O.J., Van Domburg, P.H., Ten Donkelaar, H.J. 1992. Cell loss in the nucleus raphes dorsalis in Alzheimer's disease. Neurobiology of aging 13(4), 461-8.

Assal, F., Cummings, J.L. 2002. Neuropsychiatric symptoms in the dementias. Current opinion in neurology 15(4), 445-50.

Aznavour, N., Zimmer, L. 2007. [18F]MPPF as a tool for the in vivo imaging of 5-HT1A receptors in animal and human brain. Neuropharmacology 52(3), 695-707.

Bagheri, M., Joghataei, M.T., Mohseni, S., Roghani, M. 2011. Genistein ameliorates learning and memory deficits in amyloid beta(1-40) rat model of Alzheimer's disease. Neurobiology of learning and memory 95(3), 270-6.

Beach, T.G., Sue, L.I., Walker, D.G., Sabbagh, M.N., Serrano, G., Dugger, B.N., Mariner, M., Yantos, K., Henry-Watson, J., Chiarolanza, G., Hidalgo, J.A., Souders, L. 2012. Striatal amyloid plaque density predicts Braak neurofibrillary stage and clinicopathological Alzheimer's disease: implications for amyloid imaging. Journal of Alzheimer's disease : JAD 28(4), 869-76.

Becker, G., Streichenberger, N., Billard, T., Newman-Tancredi, A., Zimmer, L. 2014. A Postmortem Study to Compare Agonist and Antagonist 5-HT1A Receptor-binding Sites in Alzheimer's Disease. CNS neuroscience & therapeutics 20(10), 930-4.

Bowen, D.M., Francis, P.T., Chessell, I.P., Webster, M.T. 1994. Neurotransmission--the link integrating Alzheimer research? Trends in neurosciences 17(4), 149-50.

Bowen, D.M., Najlerahim, A., Procter, A.W., Francis, P.T., Murphy, E. 1989. Circumscribed changes of the cerebral cortex in neuropsychiatric disorders of later life. Proceedings of the National Academy of Sciences of the United States of America 86(23), 9504-8.

Braak, H., Braak, E., Bohl, J. 1993. Staging of Alzheimer-related cortical destruction. European neurology 33(6), 403-8.

Chen, C.P., Alder, J.T., Bowen, D.M., Esiri, M.M., McDonald, B., Hope, T., Jobst, K.A., Francis, P.T. 1996. Presynaptic serotonergic markers in community-acquired cases of Alzheimer's disease: correlations with depression and neuroleptic medication. Journal of neurochemistry 66(4), 1592-8.

Cheng, K.T. 2004. 4-(2 -Methoxyphenyl)-1-[2 -(N-2 -pyridinyl)-p-[18F]fluorobenzamido]ethylpiperazine. Molecular Imaging and Contrast Agent Database (MICAD), Bethesda (MD).

Couillard-Despres, S., Winner, B., Schaubeck, S., Aigner, R., Vroemen, M., Weidner, N., Bogdahn, U., Winkler, J., Kuhn, H.G., Aigner, L. 2005. Doublecortin expression levels in adult brain reflect neurogenesis. The European journal of neuroscience 21(1), 1-14.

Cross, A.J. 1990. Serotonin in Alzheimer-type dementia and other dementing illnesses. Annals of the New York Academy of Sciences 600, 405-15; discussion 15-7.

Cross, A.J., Crow, T.J., Ferrier, I.N., Johnson, J.A. 1986. The selectivity of the reduction of serotonin S2 receptors in Alzheimer-type dementia. Neurobiology of aging 7(1), 3-7.

D'Amato, R.J., Zweig, R.M., Whitehouse, P.J., Wenk, G.L., Singer, H.S., Mayeux, R., Price, D.L., Snyder, S.H. 1987. Aminergic systems in Alzheimer's disease and Parkinson's disease. Annals of neurology 22(2), 229-36.

Dahlgren, K.N., Manelli, A.M., Stine, W.B., Jr., Baker, L.K., Krafft, G.A., LaDu, M.J. 2002. Oligomeric and fibrillar species of amyloid-beta peptides differentially affect neuronal viability. The Journal of biological chemistry 277(35), 32046-53.

de Sousa Abreu, R., Penalva, L.O., Marcotte, E.M., Vogel, C. 2009. Global signatures of protein and mRNA expression levels. Molecular bioSystems 5(12), 1512-26.

Halliday, G.M., McCann, H.L., Pamphlett, R., Brooks, W.S., Creasey, H., McCusker, E., Cotton, R.G., Broe, G.A., Harper, C.G. 1992. Brain stem serotonin-synthesizing neurons in Alzheimer's disease: a clinicopathological correlation. Acta neuropathologica 84(6), 638-50.

Hirst, W.D., Cheung, N.Y., Rattray, M., Price, G.W., Wilkin, G.P. 1998. Cultured astrocytes express messenger RNA for multiple serotonin receptor subtypes, without functional coupling of 5-HT1 receptor subtypes to adenylyl cyclase. Brain research Molecular brain research 61(1-2), 90-9.

Ishibashi, K., Ishiwata, K., Toyohara, J., Murayama, S., Ishii, K. 2014. Regional analysis of striatal and cortical amyloid deposition in patients with Alzheimer's disease. The European journal of neuroscience 40(4), 2701-6.

Kepe, V., Barrio, J.R., Huang, S.C., Ercoli, L., Siddarth, P., Shoghi-Jadid, K., Cole, G.M., Satyamurthy, N., Cummings, J.L., Small, G.W., Phelps, M.E. 2006. Serotonin 1A receptors in the living brain of Alzheimer's disease patients. Proceedings of the National Academy of Sciences of the United States of America 103(3), 702-7.

Kia, H.K., Brisorgueil, M.J., Hamon, M., Calas, A., Verge, D. 1996. Ultrastructural localization of 5-hydroxytryptamine1A receptors in the rat brain. Journal of neuroscience research 46(6), 697-708.

Klein, A.M., Kowall, N.W., Ferrante, R.J. 1999. Neurotoxicity and oxidative damage of beta amyloid 1-42 versus beta amyloid 1-40 in the mouse cerebral cortex. Annals of the New York Academy of Sciences 893, 314-20.

Klunk, W.E., Price, J.C., Mathis, C.A., Tsopelas, N.D., Lopresti, B.J., Ziolko, S.K., Bi, W., Hoge, J.A., Cohen, A.D., Ikonomovic, M.D., Saxton, J.A., Snitz, B.E., Pollen, D.A., Moonis, M., Lippa, C.F., Swearer, J.M., Johnson, K.A., Rentz, D.M., Fischman, A.J., Aizenstein, H.J., DeKosky, S.T. 2007. Amyloid deposition begins in the striatum of presenilin-1 mutation carriers from two unrelated pedigrees. The Journal of neuroscience : the official journal of the Society for Neuroscience 27(23), 6174-84.

Koivunen, J., Verkkoniemi, A., Aalto, S., Paetau, A., Ahonen, J.P., Viitanen, M., Nagren, K., Rokka, J., Haaparanta, M., Kalimo, H., Rinne, J.O. 2008. PET amyloid ligand [11C]PIB uptake shows predominantly striatal increase in variant Alzheimer's disease. Brain : a journal of neurology 131(Pt 7), 1845-53.

Lai, M.K., Tsang, S.W., Alder, J.T., Keene, J., Hope, T., Esiri, M.M., Francis, P.T., Chen, C.P. 2005. Loss of serotonin 5-HT2A receptors in the postmortem temporal cortex correlates with rate of cognitive decline in Alzheimer's disease. Psychopharmacology 179(3), 673-7.

Lai, M.K., Tsang, S.W., Francis, P.T., Esiri, M.M., Keene, J., Hope, T., Chen, C.P. 2003. Reduced serotonin 5-HT1A receptor binding in the temporal cortex correlates with aggressive behavior in Alzheimer disease. Brain research 974(1-2), 82-7.

Lanctot, K.L., Hussey, D.F., Herrmann, N., Black, S.E., Rusjan, P.M., Wilson, A.A., Houle, S., Kozloff, N., Verhoeff, N.P., Kapur, S. 2007. A positron emission tomography study of 5-hydroxytryptamine-1A receptors in Alzheimer disease. The American journal of geriatric psychiatry : official journal of the American Association for Geriatric Psychiatry 15(10), 888-98.

Le Bars, D., Lemaire, C., Ginovart, N., Plenevaux, A., Aerts, J., Brihaye, C., Hassoun, W., Leviel, V., Mekhsian, P., Weissmann, D., Pujol, J.F., Luxen, A., Comar, D. 1998. High-

yield radiosynthesis and preliminary in vivo evaluation of p-[18F]MPPF, a fluoro analog of WAY-100635. Nuclear medicine and biology 25(4), 343-50.

Lorke, D.E., Lu, G., Cho, E., Yew, D.T. 2006. Serotonin 5-HT2A and 5-HT6 receptors in the prefrontal cortex of Alzheimer and normal aging patients. BMC neuroscience 7, 36.

Maier, T., Guell, M., Serrano, L. 2009. Correlation of mRNA and protein in complex biological samples. FEBS letters 583(24), 3966-73.

Meltzer, C.C., Smith, G., DeKosky, S.T., Pollock, B.G., Mathis, C.A., Moore, R.Y., Kupfer, D.J., Reynolds, C.F., 3rd. 1998. Serotonin in aging, late-life depression, and Alzheimer's disease: the emerging role of functional imaging. Neuropsychopharmacology : official publication of the American College of Neuropsychopharmacology 18(6), 407-30.

Mizukami, K., Ishikawa, M., Akatsu, H., Abrahamson, E.E., Ikonomovic, M.D., Asada, T. 2011. An immunohistochemical study of the serotonin 1A receptor in the hippocampus of subjects with Alzheimer's disease. Neuropathology : official journal of the Japanese Society of Neuropathology 31(5), 503-9.

Mucke, L., Selkoe, D.J. 2012. Neurotoxicity of amyloid beta-protein: synaptic and network dysfunction. Cold Spring Harbor perspectives in medicine 2(7), a006338.

Nilsson, M.R. 2004. Techniques to study amyloid fibril formation in vitro. Methods 34(1), 151-60.

Noristani, H.N., Olabarria, M., Verkhratsky, A., Rodriguez, J.J. 2010. Serotonin fibre sprouting and increase in serotonin transporter immunoreactivity in the CA1 area of hippocampus in a triple transgenic mouse model of Alzheimer's disease. The European journal of neuroscience 32(1), 71-9.

Ogren, S.O., Eriksson, T.M., Elvander-Tottie, E., D'Addario, C., Ekstrom, J.C., Svenningsson, P., Meister, B., Kehr, J., Stiedl, O. 2008. The role of 5-HT(1A) receptors in learning and memory. Behavioural brain research 195(1), 54-77.

Palacios, J.M., Waeber, C., Hoyer, D., Mengod, G. 1990. Distribution of serotonin receptors. Annals of the New York Academy of Sciences 600, 36-52.

Patel, T.D., Zhou, F.C. 2005. Ontogeny of 5-HT1A receptor expression in the developing hippocampus. Brain research Developmental brain research 157(1), 42-57.

Paxinos, G., Watson, C. 2007. The rat brain in stereotaxic coordinates. 6, illustrated ed. Academic Press, 2007.

Payne, S.H. 2015. The utility of protein and mRNA correlation. Trends in biochemical sciences 40(1), 1-3.

Pike, C.J., Burdick, D., Walencewicz, A.J., Glabe, C.G., Cotman, C.W. 1993. Neurodegeneration induced by beta-amyloid peptides in vitro: the role of peptide assembly state. The Journal of neuroscience : the official journal of the Society for Neuroscience 13(4), 1676-87.

Pompeiano, M., Palacios, J.M., Mengod, G. 1992. Distribution and cellular localization of mRNA coding for 5-HT1A receptor in the rat brain: correlation with receptor binding. The Journal of neuroscience : the official journal of the Society for Neuroscience 12(2), 440-53.

Querfurth, H.W., LaFerla, F.M. 2010. Alzheimer's disease. The New England journal of medicine 362(4), 329-44.

Ramirez, M.J., Lai, M.K., Tordera, R.M., Francis, P.T. 2014. Serotonergic therapies for cognitive symptoms in Alzheimer's disease: rationale and current status. Drugs 74(7), 729-36.

Reinikainen, K.J., Soininen, H., Riekkinen, P.J. 1990. Neurotransmitter changes in Alzheimer's disease: implications to diagnostics and therapy. Journal of neuroscience research 27(4), 576-86.

Reynolds, G.P., Arnold, L., Rossor, M.N., Iversen, L.L., Mountjoy, C.Q., Roth, M. 1984. Reduced binding of [3H]ketanserin to cortical 5-ht2 receptors in senile dementia of the Alzheimer type. Neuroscience letters 44(1), 47-51.

Riad, M., Garcia, S., Watkins, K.C., Jodoin, N., Doucet, E., Langlois, X., el Mestikawy, S., Hamon, M., Descarries, L. 2000. Somatodendritic localization of 5-HT1A and preterminal axonal localization of 5-HT1B serotonin receptors in adult rat brain. The Journal of comparative neurology 417(2), 181-94.

Rodriguez, J.J., Noristani, H.N., Verkhratsky, A. 2012. The serotonergic system in ageing and Alzheimer's disease. Progress in neurobiology 99(1), 15-41.

Santarelli, L., Saxe, M., Gross, C., Surget, A., Battaglia, F., Dulawa, S., Weisstaub, N., Lee, J., Duman, R., Arancio, O., Belzung, C., Hen, R. 2003. Requirement of hippocampal neurogenesis for the behavioral effects of antidepressants. Science 301(5634), 805-9.

Sato, S., Mizukami, K., Asada, T. 2007. A preliminary open-label study of 5-HT1A partial agonist tandospirone for behavioural and psychological symptoms associated with dementia. The international journal of neuropsychopharmacology / official scientific journal of the Collegium Internationale Neuropsychopharmacologicum 10(2), 281-3.

Schechter, L.E., Smith, D.L., Rosenzweig-Lipson, S., Sukoff, S.J., Dawson, L.A., Marquis, K., Jones, D., Piesla, M., Andree, T., Nawoschik, S., Harder, J.A., Womack, M.D., Buccafusco, J., Terry, A.V., Hoebel, B., Rada, P., Kelly, M., Abou-Gharbia, M., Barrett, J.E., Childers, W. 2005. Lecozotan (SRA-333): a selective serotonin 1A receptor antagonist that enhances the stimulated release of glutamate and acetylcholine in the hippocampus and possesses cognitive-enhancing properties. The Journal of pharmacology and experimental therapeutics 314(3), 1274-89.

Selkoe, D.J. 2001. Alzheimer's disease: genes, proteins, and therapy. Physiological reviews 81(2), 741-66.

Stargardt, A., Swaab, D.F., Bossers, K. 2015. The storm before the quiet: neuronal hyperactivity and Abeta in the presymptomatic stages of Alzheimer's disease. Neurobiology of aging 36(1), 1-11.

Truchot, L., Costes, N., Zimmer, L., Laurent, B., Le Bars, D., Thomas-Anterion, C., Mercier, B., Hermier, M., Vighetto, A., Krolak-Salmon, P. 2008. A distinct [18F]MPPF PET profile in amnestic mild cognitive impairment compared to mild Alzheimer's disease. NeuroImage 40(3), 1251-6.

Truchot, L., Costes, S.N., Zimmer, L., Laurent, B., Le Bars, D., Thomas-Anterion, C., Croisile, B., Mercier, B., Hermier, M., Vighetto, A., Krolak-Salmon, P. 2007. Up-regulation of hippocampal serotonin metabolism in mild cognitive impairment. Neurology 69(10), 1012-7.

Verdurand, M., Berod, A., Le Bars, D., Zimmer, L. 2011. Effects of amyloid-beta peptides on the serotoninergic 5-HT1A receptors in the rat hippocampus. Neurobiology of aging 32(1), 103-14.

Villemagne, V.L., Ataka, S., Mizuno, T., Brooks, W.S., Wada, Y., Kondo, M., Jones, G., Watanabe, Y., Mulligan, R., Nakagawa, M., Miki, T., Shimada, H., O'Keefe, G.J., Masters, C.L., Mori, H., Rowe, C.C. 2009. High striatal amyloid beta-peptide deposition across different autosomal Alzheimer disease mutation types. Archives of neurology 66(12), 1537-44.

Vogel, C., Marcotte, E.M. 2012. Insights into the regulation of protein abundance from proteomic and transcriptomic analyses. Nature reviews Genetics 13(4), 227-32.

Whitaker-Azmitia, P.M., Clarke, C., Azmitia, E.C. 1993. Localization of 5-HT1A receptors to astroglial cells in adult rats: implications for neuronal-glial interactions and psychoactive drug mechanism of action. Synapse 14(3), 201-5.

Wu, Q.Y., Li, J., Feng, Z.T., Wang, T.H. 2007. Bone marrow stromal cells of transgenic mice can improve the cognitive ability of an Alzheimer's disease rat model. Neuroscience letters 417(3), 281-5.

Zheng, M., Liu, J., Ruan, Z., Tian, S., Ma, Y., Zhu, J., Li, G. 2013. Intrahippocampal injection of Abeta1-42 inhibits neurogenesis and down-regulates IFN-gamma and NF-kappaB expression in hippocampus of adult mouse brain. Amyloid : the international journal of experimental and clinical investigation : the official journal of the International Society of Amyloidosis 20(1), 13-20.

Zweig, R.M., Ross, C.A., Hedreen, J.C., Steele, C., Cardillo, J.E., Whitehouse, P.J., Folstein, M.F., Price, D.L. 1988. The neuropathology of aminergic nuclei in Alzheimer's disease. Annals of neurology 24(2), 233-42.

Aβ40

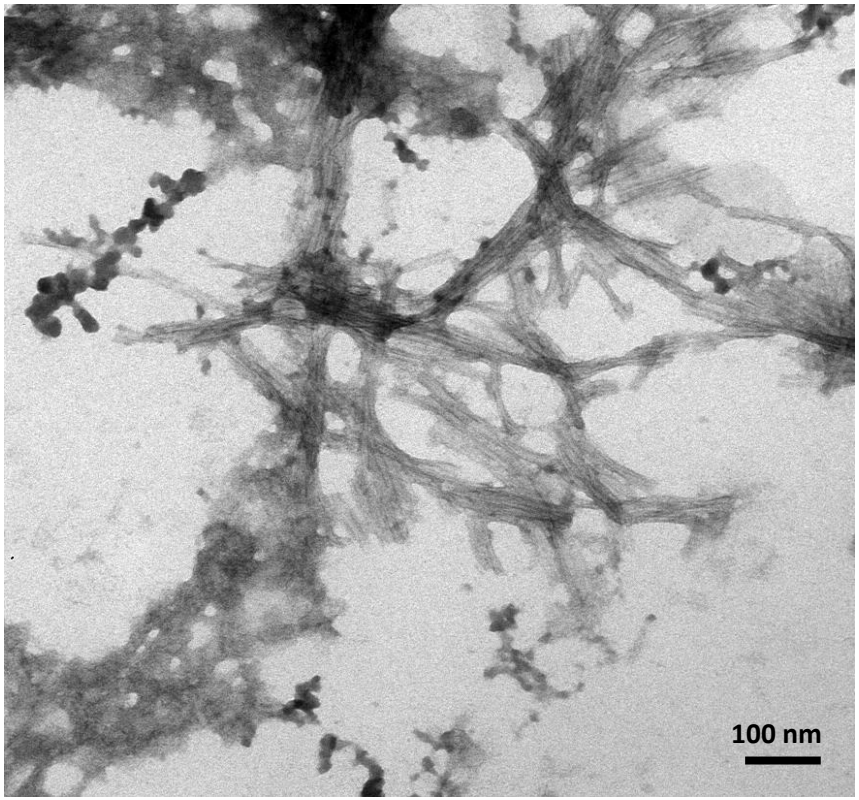

Aβ42

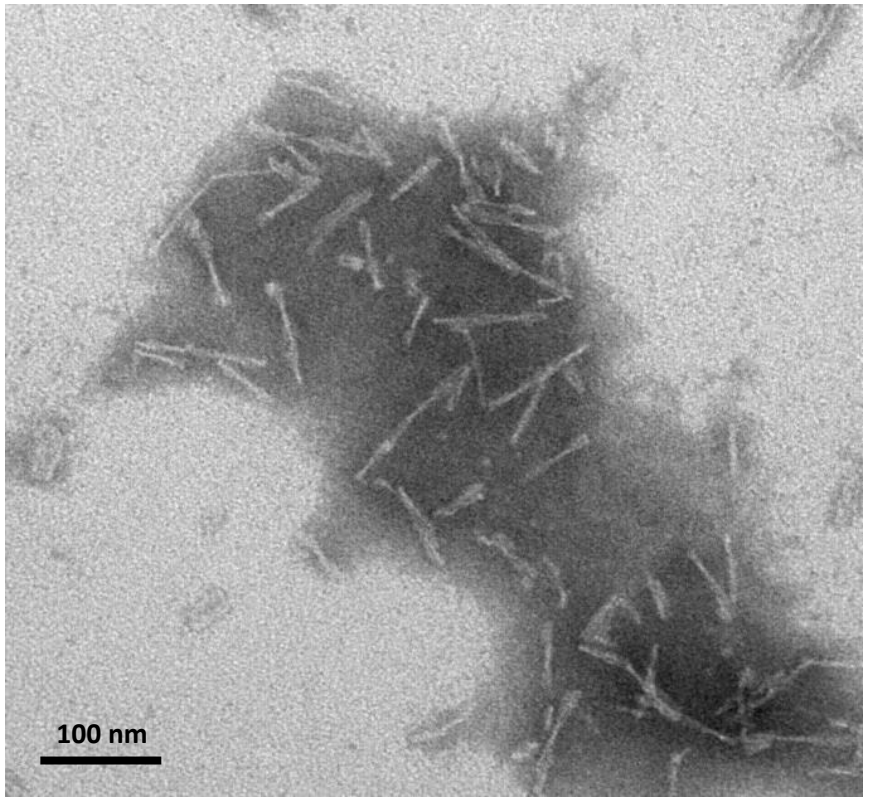

Hippocampus

vehicle Aβ

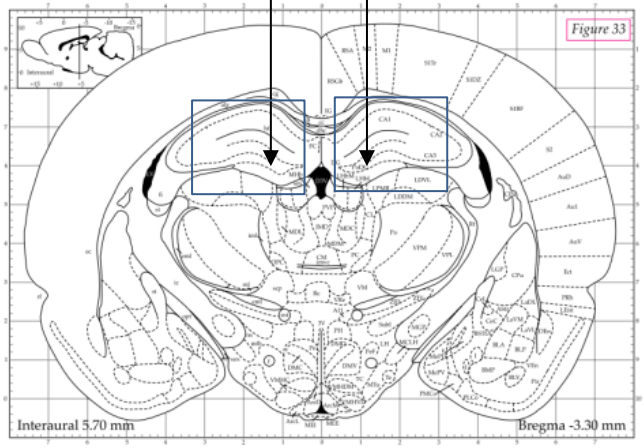

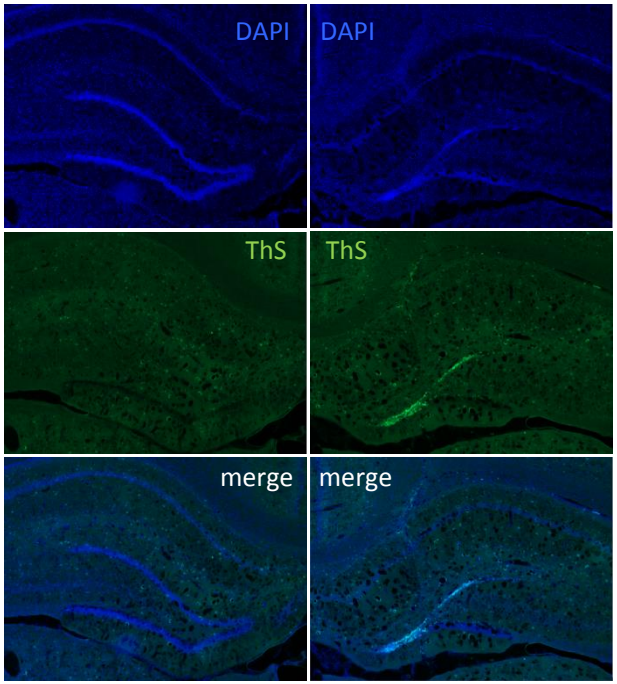

Striatum

vehicle Aβ

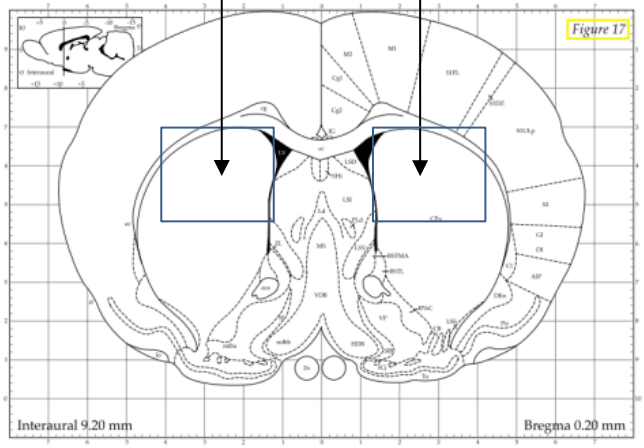

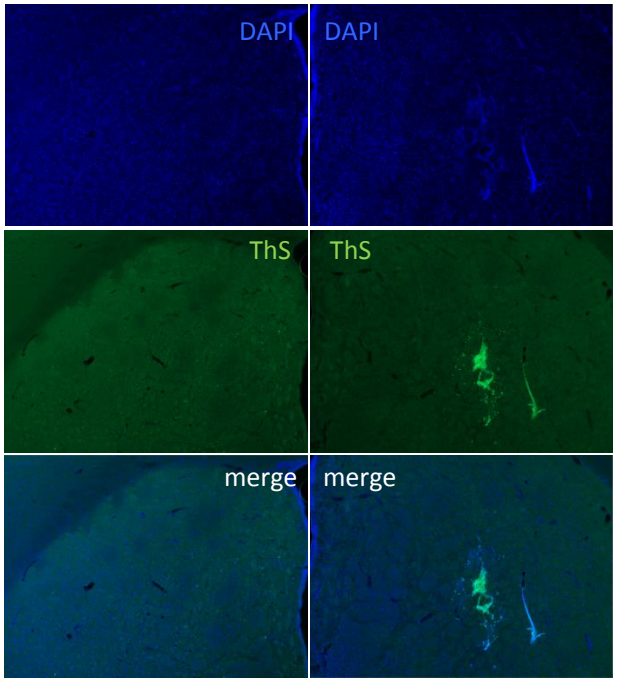

Dentate Gyrus

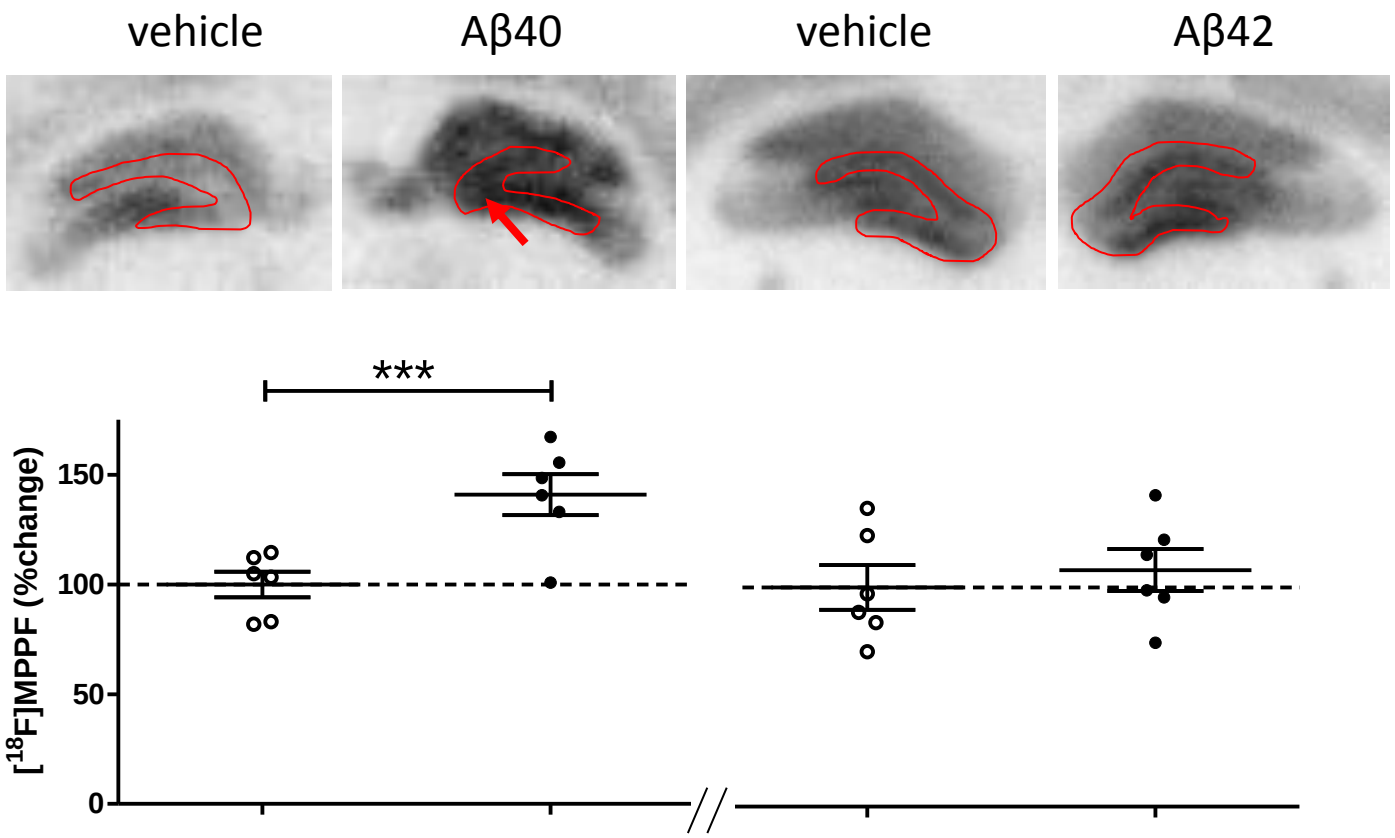

Striatum

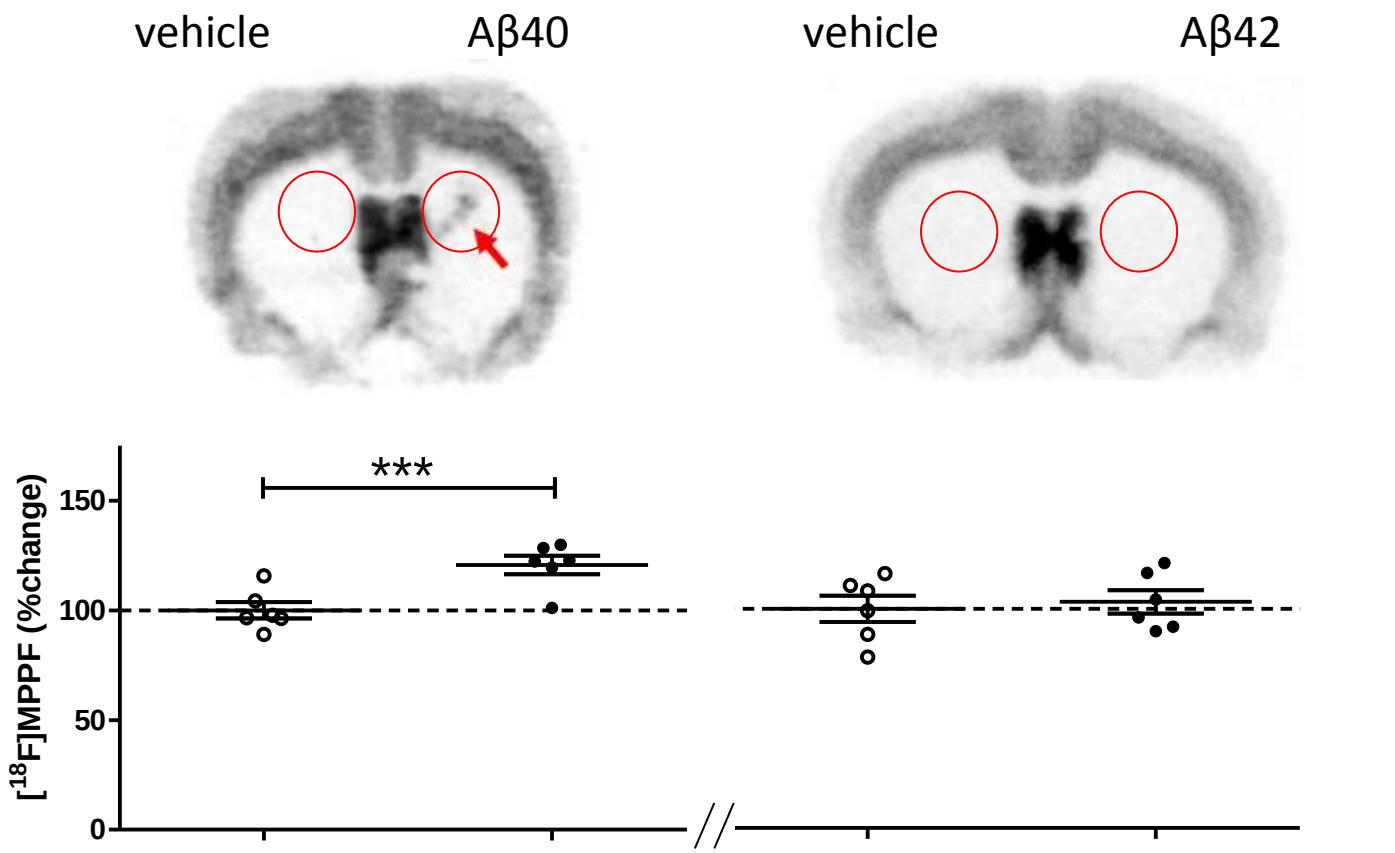

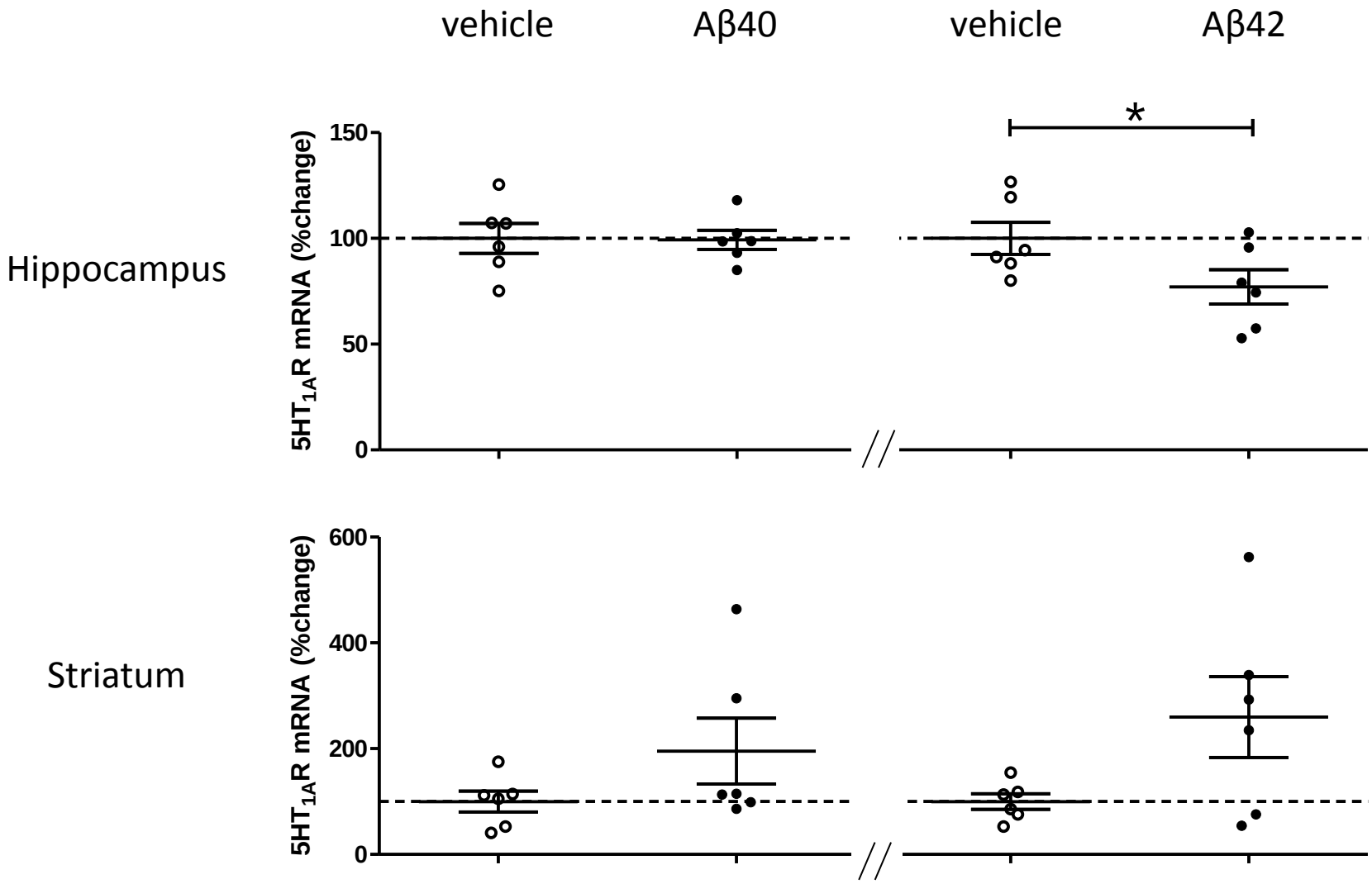
vehicle
Aβ40
vehicle
Aβ42
*
Hippocampus
Striatum
5HT1AR mRNA (%change)
150
100
50
0
600
400
200
0

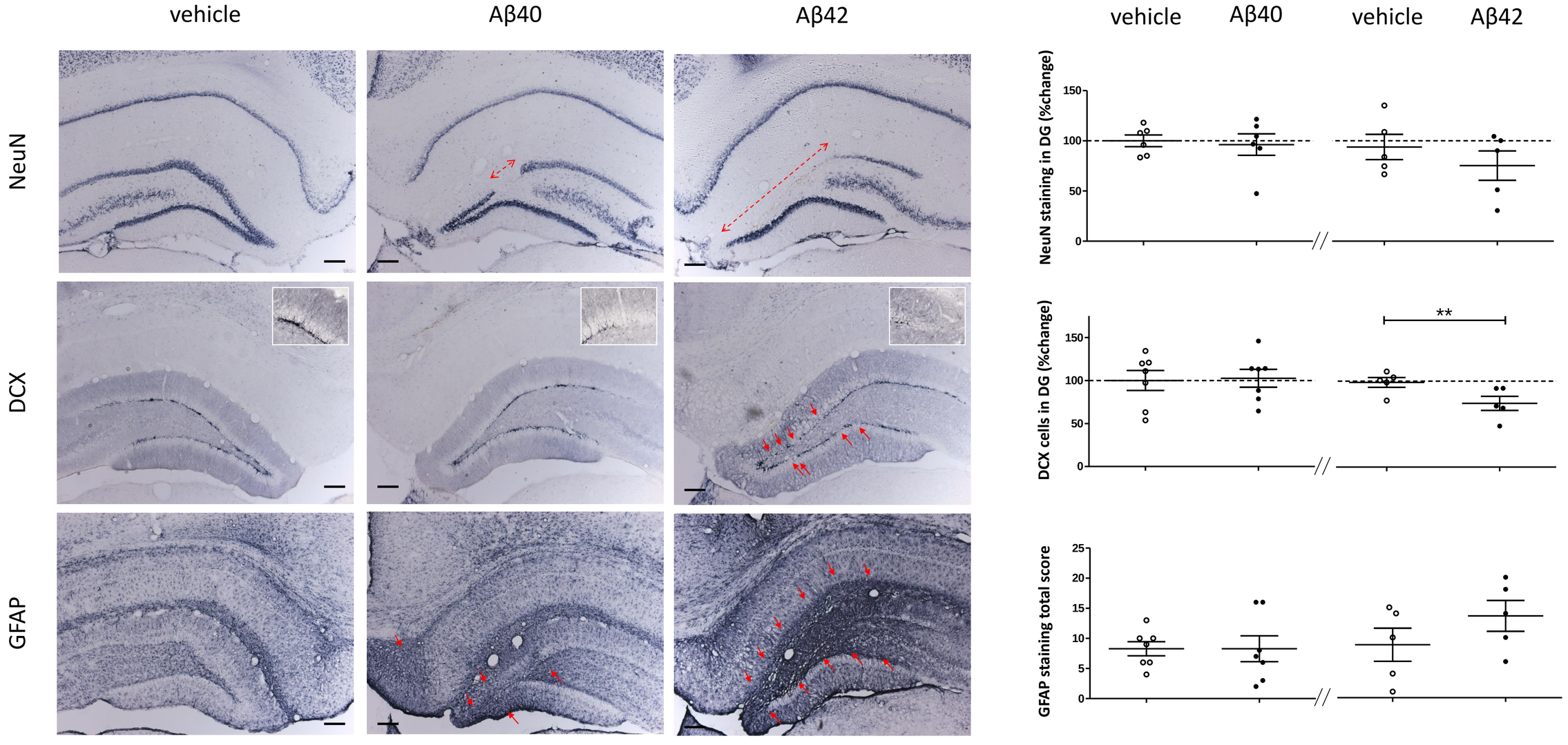
vehicle
Aβ40
Aβ42
NeuN
DCX
GFAP
vehicle
Aβ40
vehicle
Aβ42
NeuN staining in DG (%change)
150
100
50
0
DCX cells in DG (%change)
**
GFAP staining total score
25
20
15
10
5
0

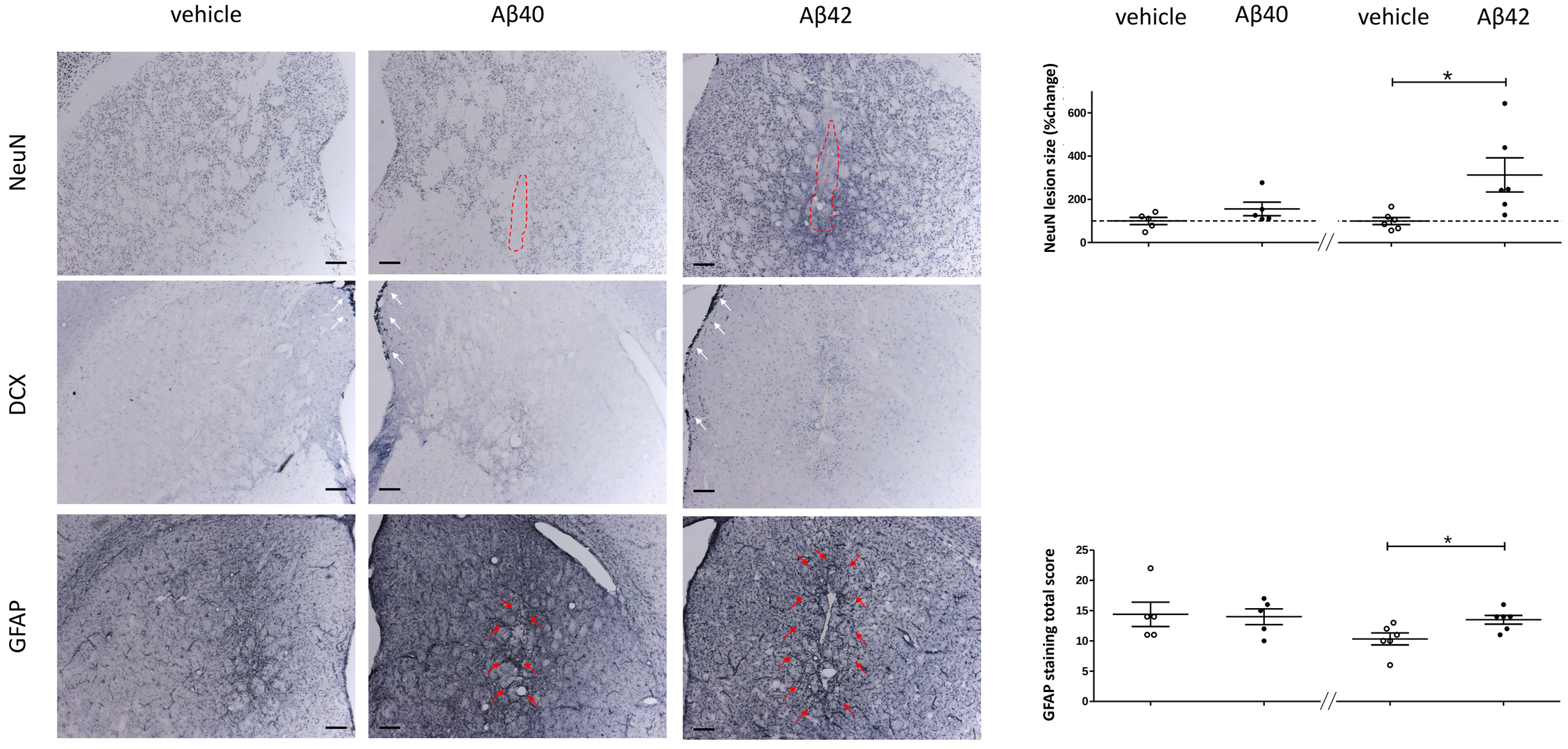
vehicle
Aβ40
Aβ42
NeuN
DCX
GFAP
vehicle
Aβ40
vehicle
Aβ42
NeuN lesion size (%change)
0
200
400
600
*
GFAP staining total score
0
5
10
15
20
25
*

Highlights.

- Neurodegenerative processes have effects on serotonergic neurotransmission
- Aβ40 fibrils, but not Aβ42, can trigger an overexpression of 5-HT_{1A}R in rat brain
- Aβ42 fibrils are more neurotoxic than Aβ40 *in vivo*
- Aβ42 fibrils decrease neurogenesis in the hippocampus